Electron Accumulation on Metal Nanoparticles in Plasmon-Enhanced Organic Solar Cells

Michael Salvador, Bradley A. MacLeod,[†] Angela Hess, Abhishek P. Kulkarni,[‡] Keiko Munechika,[§] Jennifer I. L. Chen,[⊥] and David S. Ginger*

Department of Chemistry, University of Washington, Seattle, Washington 98195-1700, United States

ABSTRACT Plasmonic metal nanoparticles have been used to enhance the performance of thin-film devices such as organic photovoltaics based on polymer/fullerene blends. We show that silver nanoprisms accumulate long-lived negative charges when they are in contact with a photoexcited bulk heterojunction blend composed of poly(3-hexylthiophene)/phenyl-C61-butyric acid methyl ester (P3HT/PCBM). We report both the charge modulation and electroabsorption spectra of silver nanoprisms in solid-state devices and compare these spectra with the photoinduced absorption spectra of P3HT/PCBM blends containing silver nanoprisms. We assign a previously unidentified peak in the photoinduced absorption spectra to the presence of photoinduced electrons on the silver nanoprisms. We show that coating the nanoprisms with a 2.5 nm thick insulating layer can completely inhibit this charging. These results may inform methods for limiting metal-mediated losses in plasmonic solar cells.

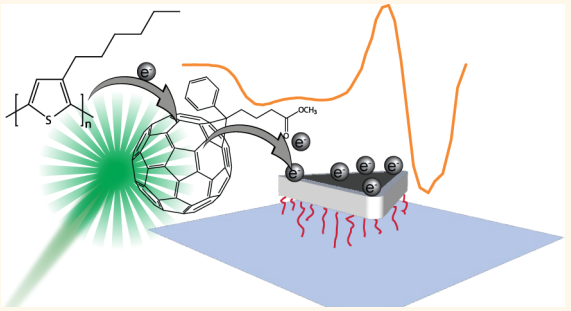

KEYWORDS: localized surface plasmon resonance · metal nanoparticles · electron transfer · charge-induced plasmonic shift · light trapping · plasmon-enhanced solar cells · organic bulk heterojunction

Plasmon-resonant metal nanoparticles have been used to enhance the performance of optoelectronic devices such as LEDs,[1] lasers,[2] photodiodes,[3] and biosensors,[4] because the redistribution of electromagnetic field modes around the metal particles enhances absorption,[5,6] emission,[7−11] and Raman scattering[12,13] and even leads to apparent violations of Kasha's rules of molecular photophysics.[14] In particular, plasmonic nanoparticles are of interest for light management in thin-film solar cells because they can be used to increase the amount of light absorbed in an active semiconductor layer through electromagnetic near-field enhancement, far-field scattering (increase in path length), and plasmonic waveguiding depending on the circumstances.[15,16] Plasmonic light harvesting can be beneficial for organic photovoltaics in particular, because many of the current generation of materials exhibit decreasing internal quantum efficiency (IQE) with increasing film thickness.[17,18] Recently, the combined effects of incorporating plasmonic metal nanoparticles and a nanostructured metal back electrode resulted in a single-junction organic solar cell featuring a power conversion efficiency of 8.8%, which is among the highest values reported in the literature.[19]

Enhanced light harvesting using plasmon-resonant metal nanoparticles is thus one promising route to improve light absorption in optically thin organic photovoltaic (OPV) films with high IQEs, while perhaps alleviating some of the challenges associated with optimizing organic blend morphology. Metal nanoparticles can be assembled from solution, and colloidal synthesis methods allow spectral tunability of the metal particle plasmons,[20] opening the way toward a scalable low-cost solution processed platform for plasmonic OPVs with a range of tailored materials. Despite these seeming advantages, there are potential challenges to the successful incorporation of metal nanoparticles in organic photovoltaics. Because the near-field enhancement is large in close vicinity to the particle but decays quickly within a few tens of nanometers, the particles

* Address correspondence to ginger@chem.washington.edu.

Received for review August 16, 2012 and accepted October 14, 2012.

Published online October 14, 2012
10.1021/nn303725v

ideally should be embedded into the active OPV layer.[21] However, redispersion of metal nanoparticles, especially anisotropic particles, in the halogenated organic solvents commonly used for preparing OPV blend films is rather inefficient and can lead to rapid shape changes.[22] Furthermore, bare metal nanoparticles may promote charge recombination and exciton quenching losses at the metal surface due to dipole–dipole and charge-trapping mechanisms, making it necessary to isolate the particle with a thin dielectric layer.[23,24]

Recently, plasmonic effects have been used in numerous studies to enhance the performance of organic bulk heterojunction solar cells.[16,19,24–36] Because the majority of those studies have focused primarily on the overall device efficiency, the mechanisms underlying these performance changes are not always clear. For instance, some studies suggest that the inclusion of metal nanoparticles may affect both open-circuit voltage (V_{OC})[26,31] and fill factor (FF),[27,34] while others report improved charge carrier mobility in addition to enhanced charge carrier generation.[19,24,28] Some of these effects are surprising, as the optical effect of the nanoparticles should be primarily to increase only the photocurrent density as a result of enhanced absorption in the photovoltaic layer. The observation of improved FF in combination with metal nanoparticle enhanced OPVs may originate from enhanced electrode roughness or morphological changes, leading to larger internal surface areas and, therefore, improved charge carrier extraction, while a larger V_{OC} can arise from electronic interaction (altered pinning effects) or chemical reaction at the metal/polymer interface.[19,26,31] In fact, a recent Raman study of the interaction of plasmonic metal nanoparticles with PEDOT:PSS suggests that silver nanoparticles facilitate photoinduced chemical changes to the polymer electrode, which contribute to the enhancement of solar cell performance.[37] In some cases, the metal nanoparticles may simply form an additional transportation network, thereby improving the electrical conductivity of the OPV layer.[24,38] Note that negative results, *i.e.*, reduced power conversion efficiency and minor, often not understood effects, have also been reported.[24,39] Hence, a fundamental understanding of the exact mechanisms of efficiency enhancement (or reduction) is an important prerequisite for engineering light-trapping strategies in thin-film solar cells using metal nanoparticles.

In a recent study, we showed that plasmon-resonant silver nanoprisms indeed have the potential to enhance the performance of OPVs by plasmonic absorption enhancement in polymer/fullerene bulk heterojunction blends.[29] To remove the ambiguity associated with device measurements, we used photoinduced absorption spectroscopy to directly measure the concentration of long-lived photogenerated charge carriers on the conjugated polymer, and we found that the plasmonic particles could increase the photogeneration of carriers by a factor of 3. On the other hand, we also found that the photoinduced absorption spectrum of the P3HT/PCBM blend showed a new feature around the peak of the silver nanoprisms' localized surface plasmon resonance. We speculated that this feature might be associated with the transfer of negative charge to the silver particles, although we were unable to test this hypothesis.

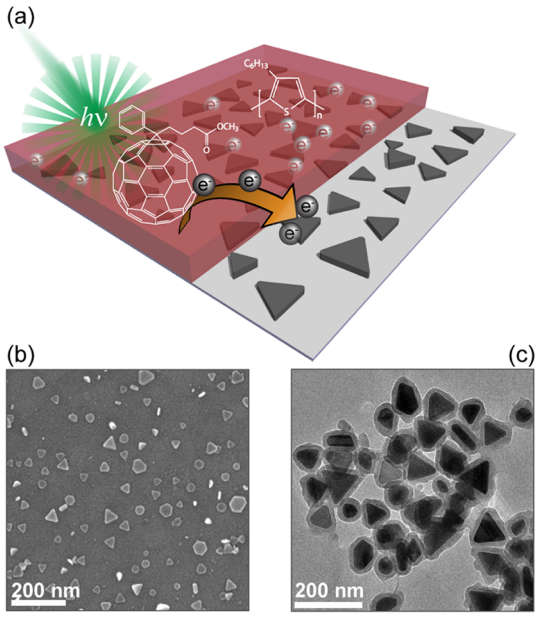

Figure 1. (a) We report on electron accumulation on metal nanoparticles following photoinduced electron transfer. This process can lead to charge recombination or enhanced electron harvesting in plasmonic solar cells, depending on the circumstances. Plasmon-enhanced organic photovoltaic active layers with tunable plasmon resonance were fabricated by depositing silver nanoprisms on glass or ITO using nanoprisms both without (b) and with (c) a silica coating. (b) SEM micrograph of bare prisms on ITO. (c) The nanoprisms can also be insulated with silica shells of varying thickness; the image shows a TEM micrograph of silica-coated silver nanoprisms with a silica coating averaging 18 nm in thickness.

Because such charge transfer processes to the metal particles could have important implications for recombination loss in plasmon-enhanced OPVs, we now address these questions by combining optical and electrical measurements using both photoinduced absorption[29,40] and charge-modulated spectroscopy.[41,42] We demonstrate that upon photoexcitation, silver nanoprisms accumulate negative charge, leading to a blue shift of the silver nanoprism plasmon resonance (Figure 1). In a plasmonic OPV device, this could represent a path for charge recombination and possibly affect V_{OC} and charge carrier extraction. To prevent electron charging of the silver particles, we present two very different approaches: inclusion of a dielectric layer between nanoprisms and organic blend and growing of a protective silica shell around the nanoprism by chemical means (Figure 1). Both approaches show that only a few nanometers of dielectric shell material is required to inhibit the observed electron transfer to the silver nanoprisms.

RESULTS AND DISCUSSION

We study films of the bulk heterojunction organic photovoltaic blend P3HT/PCBM in contact with silver

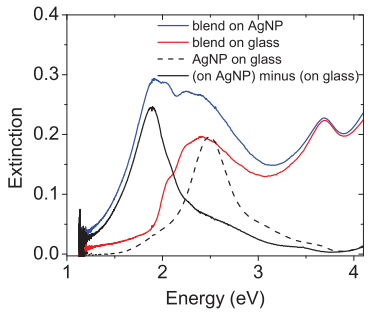

Figure 2. Extinction spectra of 35 nm thick P3HT/PCBM blend films coated onto bare glass (red line) and on top of silver nanoprisms on glass (blue line). The black dotted line shows the extinction spectrum of the bare silver nanoprisms on glass, while the black solid line is the difference between the extinction spectra of the polymer blend on bare glass and the polymer blend on the nanoprisms. The red shift of the nanoprisms' extinction upon coating with the polymer blend results primarily from the increased refractive index of the polymer blend compared with air.

nanoprisms, as have been previously shown to enhance photoinduced carrier generation.[29] Figure 2 shows extinction (scattering + absorption) spectra of silver nanoprisms immobilized on glass as well as the same film after being overcoated with a 35 nm thick layer of a 1:1 P3HT/PCBM blend. We estimate the spectrum of the nanoprisms under the blend by subtracting the bare blend spectrum from the sample glass/silver nanoprism/blend (Figure 2). Figure 2 shows that overcoating the particles with the polymer blend generally causes the plasmon resonance to red shift by ~0.6 eV and the extinction increases by 20%. Both effects are qualitatively consistent with changes resulting from the increase in the local refractive index due to the polymer film.[43] While a more detailed analysis might also separate absorption enhancement and coupling effects in the difference spectrum, such an analysis is not the focus of this article.

When photoexcited, the polymer/fullerene blend generates long-lived charge carriers as a result of photoinduced charge transfer from the P3HT donor to the PCBM acceptor.[40,44] The positive polarons on the polymer in particular have a strong IR absorption that peaks around 1.25 eV, permitting spectroscopic measurement of photocarrier generation.[29,45]

Figure 3a shows photoinduced absorption spectra of both a plain P3HT/PCBM blend and a P3HT/PCBM blend coated on top of a dense silver nanoprism film, whose extinction spectrum inside the polymer blend is displayed in Figure 3b. As expected, both films exhibit a strong polaron absorption feature at ~1.25 eV (Figure 3a). Consistent with previous work, the intensity of the polaron absorption feature is considerably enhanced for the blend in the presence of the silver nanoprisms as a result of near-field absorption enhancement of the pump light.[29] In addition to the enhanced polaron yield evident at 1.25 eV, the photoinduced absorption spectrum for the blend

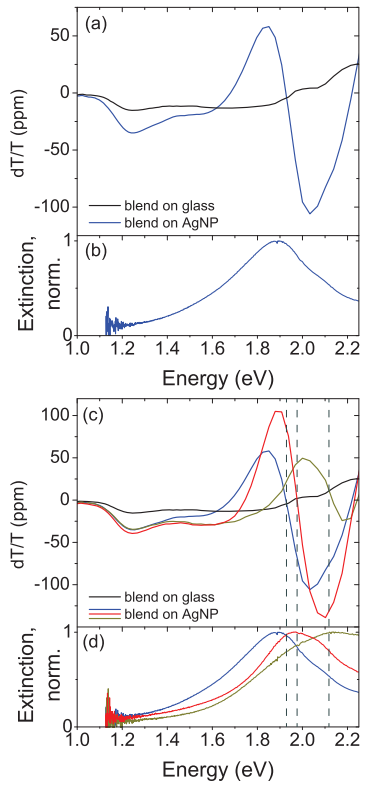

Figure 3. (a) Photoinduced absorption spectra (530 nm pump LED) of P3HT/PCBM films on top of glass (black line) and on top of a self-assembled monolayer of silver nanoprisms (AgNPs, blue line). Note that negative dT/T values mean an increase in absorption, while positive dT/T values represent an increase in transmission (bleach). (b) Estimated extinction spectrum of the silver nanoprism layer shown in (a) embedded in the polymer blend (blend on AgNP minus blend on glass). The panels (c) and (d) are analogous to (a) and (b) using silver nanoprism batches with different plasmon resonances. The dashed vertical lines are guides to the eye showing the relation between the derivative line shape of the AgNP's photoinduced aborption signal and its extinction spectrum.

coated on top of the nanoprisms exhibits an intense new feature with a new absorption at 2.03 eV and a concomitant bleach at 1.85 eV.

This paired bleach/absorption feature is clearly associated with the silver nanoprisms in contact with the bulk heterojunction blend. All three components—nanoprisms, P3HT, and PCBM—must be present for the new feature to be observed (see Supporting Information, Figure S1). Notably, Figure 3c, d show that the position of the absorption and bleach shifts along with the peak of the plasmon resonance for different silver nanoprism samples featuring different average particle sizes. Comparing the photoinduced absorption spectra for the different nanoprism samples in Figure 3c, d, we see that the inflection point of the new feature occurs at almost exactly the peak of the plasmon resonance (dashed lines Figure 3c, d; see also Figure S2).

The dependence of the photoinduced absorption signal intensity on pump modulation frequency can be used to determine the lifetime of the excited species.[45,46] Figure 4 shows the modulation dependence

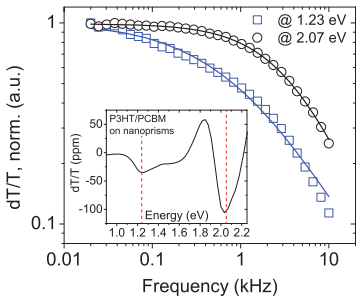

Figure 4. Pump modulation frequency dependence of the photoinduced absorption signal at 1.23 eV (squares) and 2.07 eV (circles) for a 35 nm P3HT/PCBM film on top of a silver nanoprism monolayer (530 nm pump LED) along with fit curves. In both cases, the symbols represent experimental data, while the solid lines are fits to a dispersive lifetime equation (see Supporting Information).[46] The tau parameter of the polaron signal at 1.23 eV is ~0.19 ms, while the plasmon feature associated with the silver nanoprisms at 2.07 eV has a shorter tau parameter of ~0.04 ms. The inset shows the corresponding photoinduced absorption spectrum of the same sample and the spectral positions at which the modulation dependence was recorded (dashed lines).

of the polymer polaron peak (at 1.23 eV) and the feature associated with the nanoprisms at 2.07 eV. The modulation dependence is clearly different at the two energies. The signal at 1.23 eV falls off faster with increasing modulation frequency, implying a longer average lifetime for the polaron. We also fitted the modulation frequency data to a parametric dispersive lifetime model[46] (see Supporting Information). The fit parameter τ, which is associated with the relaxation time of the excited species, is 0.19 and 0.04 ms for the 1.23 and 2.07 eV excitations, respectively, indicating that these features arise from different species. While the τ values are essentially fit parameters, the trend for the extracted τ values is consistent with the "knee" of the modulation dependency curves moving to higher frequency (shorter relaxation time)[47] again indicating that the polymer polaron feature has a longer lifetime than the nanoprism-associated plasmon feature.

On the basis of the derivative-like line shape of the nanoprisms' photoinduced absorption feature, it appears that the plasmon feature arises from a photoinduced blue shift of the nanoprism plasmon resonance peak position upon photoexcitation of the blend (Figure S3). One possibility is that the photoexcitation of charges in the polymer/fullerene matrix changes the refractive index of the polymer blend, which leads to a shift in the nanoprisms' plasmon resonance peak. We rule out such a host matrix refractive index change as the cause of the feature for two reasons. First, a Kramers–Kronig transform[48] of the photoinduced absorption data shows that any photoinduced refractive index changes of the P3HT/PCBM blend should lead to an *increase* in its refractive index in the spectral region around the plasmon peak and hence a derivative feature of opposite sign of that seen in our experiments (Supporting Information, Figure S4). Second, as noted above, the lifetime of the nanoprism spectral feature is different from that of the polymer polaron (Figure 4), suggesting that the nanoprism feature cannot result only from the nanoprism reacting passively to the changes in carrier density/refractive index on the polymer (as such an effect would exhibit the same lifetime as the polymer polarons).

To investigate the origins of the plasmonic feature further, we used a combination of electroabsorption and charge modulation spectroscopy experiments to test whether the feature is consistent with a blue shift in the plasmon resonance of the nanoprisms due to long-lived electrons injected into the silver nanoprisms. We performed electroabsorption and charge modulation spectroscopies on the silver nanoprisms using a variety of solid-state device structures to permit electrical charging (for charge modulation spectroscopy) or the application of electrical fields without charge injection (for electroabsorption spectroscopy controls). Figure 5a shows the device geometries we used. They consisted of transparent indium tin oxide (ITO) electrodes, thermally evaporated SiO_X insulators, and silver nanoprism films attached to the oxide *via* silane (APTMS) coupling (see Experimental Methods for full fabrication details).[29,49] SiO_X was deposited by thermal evaporation of SiO. The electroabsorption/charge modulation experiment is described more fully in the Supporting Information of ref 41.

The first structure shown in Figure 5a (structure A) is a control sample consisting of ITO/SiO_X/silver nanoprisms/SiO_X/Al, where silver nanoprisms are sandwiched between SiO_X layers, preventing charging of silver nanoprisms from both electrodes, while allowing an electrical field to be applied across the device. The electroabsorption spectrum in Figure 5b (orange line) shows that samples of this type do not show the characteristic line shape observed at the plasmon peak position in the photoinduced absorption experiments under typical experimental conditions.

To study the more interesting case of charge injection to/from the prisms, we utilized capacitor structures of the form ITO/silver nanoprisms/SiO_X/Al with silver nanoprisms in electrical contact with the ITO (Figure 5a, structure B). Structure B allows charge injection directly into the prisms, whereas structure A is a control to separate electric field effects from carrier injection.

When charge is injected from the ITO into the prisms, the charge modulation spectrum (Figure 5b, blue line) shows a derivative-like line shape very similar to that observed in the photoinduced absorption spectra. In contrast, the control structure (A) with an insulator blocking charge injection shows almost no signal (Figure 5b, orange line), arguing against strong electroabsorption (Stark) effects as the origin of the nanoprism feature. As in the case of the photoinduced absorption feature, the inflection point of the dT/T

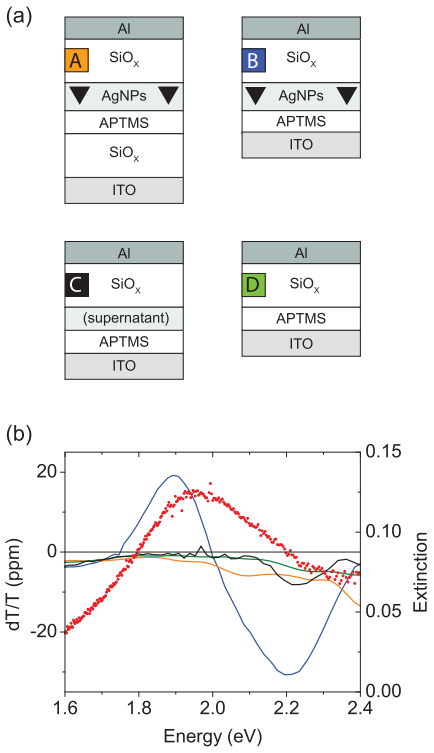

Figure 5. (a) Device structures that were analyzed using electroabsorption (structure A) and charge modulation spectroscopy (structures B, C, D). The SiO_X layer was 200 nm, and the Al top electrode is 100 nm thick in all cases. (b) Extinction spectrum of silver nanoprisms inside the structure ITO/silver nanoprism/SiO_X (red dots) and electroabsorption/charge modulation spectra for all structures shown in (a). The color codes are the same as those used within the labels of the device structures.

signal in the charge modulation spectra appears at the maximum of the plasmon resonance (1.95 eV), which is also shown in Figure 5b (red dots). We also measured charge-modulated transmittance spectra of two control structures in the absence of silver nanoprisms: (C) ITO/supernatant/SiO_X/Al (Figure 5b, black line), where APTMS-coated ITO was immersed in the supernatant of a colloidal silver solution, and (D) ITO/SiO_X/Al (Figure 5b, green line). None of the control samples showed the characteristic derivative line shape. These controls allow us to rule out the possibility that other components of the blends or solutions or that extrinsic effects are associated with the observed charge modulation experiment under applied bias. Additionally, we performed charge modulation experiments on ITO/silver nanoprism/SiO_X/Al structures containing several different sizes of silver nanoprisms. As expected, the silver nanoprisms' charge modulation spectra tracked consistently with the changing position of the plasmon resonance (Figure S7).

Importantly, we can use the sign and phase of the charge modulation signal to determine whether electrons are being either injected or collected through the ITO electrode and, consequently, whether the silver nanoprisms are either reduced or oxidized during photoexcitation (see also Supporting Information). When the ITO is biased negatively (electrons are injected), we see a bleach emerging to the red and a charge-induced absorption to the blue of the silver plasmon peak (Figures 5b and S7). This feature has the same sign and shape as the one observed in the photoinduced absorption spectra and indicates that the spectroscopic fingerprint in the range above 1.6 eV in the charge modulation spectrum is due to a blue shift of the silver nanoprism plasmon resonance as a response to charging of the silver nanoprisms by electron injection onto the nanoprisms. Since this fingerprint matches that seen in the photoinduced absorption spectra, we conclude that electron injection into the nanoprisms following photoexcitation of the polymer/fullerene blend is consistent with the nanoprism-associated peak we observe in the photoinduced absorption spectra.

These measurements are in good agreement with both theoretical expectations[50] and previous work on electrochemical charging of plasmonic nanostructures where blue- and red-shifted plasmon resonances have been observed in spherical metal nanoparticles depending on the potential applied and whether electrons were injected or withdrawn, respectively.[51−53] Charge injection into the nanoprisms is expected to cause a charge-induced plasmonic shift due to changes in the free electron density (N). At the most basic level, increasing the electron density of the metal nanoparticle will increase the plasma resonance frequency (ω_p); that is, electron injection shifts the plasmon resonance to a higher energy ($\omega_p^2 = Ne^2/\varepsilon_o m_e$, e is the charge of an electron, m_e is the effective mass of an electron, ε_o is the vacuum permittivity).[50,54]

We now return to the frequency modulation data in Figure 4. The data indicate that photogenerated electrons from the P3HT/PCBM film are being transferred to the silver nanoprisms and that these electrons are residing on the nanoprisms for relatively long times. Interestingly, the measured lifetime of the electron on the nanoprisms is shorter than the lifetime of the hole on the polymer, suggesting that there is an unobserved intermediate species involved in recombination (possibly return of the electron to a fullerene domain). Furthermore, the lifetime of the hole polarons on the polymer (~0.2 ms) is fairly insensitive to the presence or absence of the nanoprisms (Supporting Information, Figure S5). This result in itself is quite surprising. It suggests that, at least in these films, the hole lifetime is not dramatically altered by possible recombination paths with the excess electrons on the nanoprisms, which might mean that it is possible to harvest the electrons transferred to the nanoprisms at the cathode of a photodiode. This result would be consistent with suggestions that some of the improved performance (such as increases in fill factors) of metal nanoparticle/organic photovoltaic blends is not entirely plasmonic in nature, but results from an increase in charge

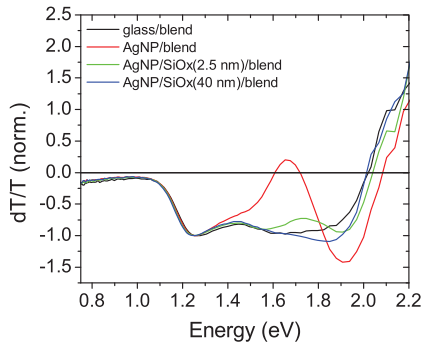

Figure 6. Normalized photoinduced absorption spectra of P3HT/PCBM blend films (35 nm) on glass (black line) and on silver nanoprisms (red line). When the silver nanoprisms and the polymer blend are separated by a dielectric layer of SiO_X (2.5 nm, green line; 40 nm, blue line), the photoinduced absorption feature resulting from electron transfer to the silver nanoprisms disappears (455 nm pump LED).

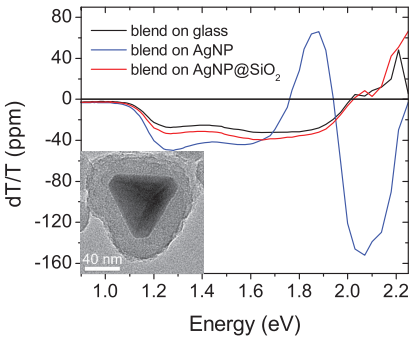

Figure 7. Photoinduced absorption spectra of the polymer blend on glass (black line) and on silver nanoprisms (blue line). Electron transfer to the silver nanoprisms is inhibited when the particles are coated with a silica shell (red line). The inset shows a TEM image of a silica-coated silver nanoprism (AgNP@SiO_2) (530 nm pump LED).

collection efficiency to the electrodes.[19,24,38] While such processes might be beneficial, the presence of bare metal nanoparticles in a device structure under operating conditions could in general lead to additional loss or shorting pathways not evident in an all-optical experiment such as those described herein.

Finally, we examine the effects of coating the silver nanoprisms with insulating shells to prevent them from coming into direct electrical contact with the semiconducting P3HT/PCBM layer. We use both evaporated SiO_X layers and silica shells grown by solution methods.[55,56] Figure 6 compares photoinduced absorption spectra for samples with and without a SiO_X layer on top of the silver nanoprism monolayer. The spectra are normalized to the amplitude of the polaron signal (1.25 eV) to allow for comparison of the spectral shapes. The plain P3HT/PCBM film shows the characteristic polaronic absorption features. The P3HT/PCBM samples with bare silver nanoprisms underneath the polymer blend feature both the expected polaronic absorption and the nanoprism-photoinduced derivative-like feature at ~1.8 eV. When the nanoparticles and the blend are separated by a thin SiO_X film, the silver nanoprisms' photoinduced absorption signature disappears and the spectrum resembles that of a bare P3HT/PCBM film. Notably, the experiment shows that only a very thin layer of 2.5 nm is required to prevent most of the electron transfer to the silver nanoprisms.

We obtained similar results by chemically growing a dielectric silica shell around the particles.[55,56] Figure 7 compares photoinduced absorption spectra for polymer blend samples with and without silica-coated silver nanoprism films underneath. From the disappearance of the nanoparticle plasmon feature in the case of silica-protected particles we conclude that electron transfer to the silver nanoprisms is turned off by the silica shell. From TEM images (Figure 7, inset) we estimated the average silica shell thickness to be ~20 nm. Despite the relatively thick silica shell, polymer blend films on top of silica-protected nanoprisms show modest polaron yield enhancements of up to 20%, perhaps due to some contributions from areas where the shells are thinner or from far-field scattering.

CONCLUSION

Using charge modulation spectroscopy, we showed that the new photoinduced absorption feature that appears in plasmon-enhanced organic photovoltaic blends under illumination is consistent with the presence of *ca.* millisecond-lived electrons that are transferred to the metal nanoparticles in the film. This process could represent both an opportunity to improve electron harvesting in blends where electron mobility is limiting and a potential recombination loss mechanism, depending on the exact device and film properties. We imagine that charge transfer to the metal is likely to be disadvantageous in the most efficient devices, and we confirmed spectroscopically that a thin dielectric layer is sufficient to completely suppress the electron transfer without turning off the plasmonic enhancement of the charge generation. Chemically grown silica shells around metal nanoparticles thus represent a promising approach for achieving plasmon-mediated charge carrier enhancements while preventing recombination losses in organic solar cells.

EXPERIMENTAL METHODS

Silver Nanoprism Synthesis. For the silver nanoprism synthesis we followed the photoinduced conversion with pH control procedure described by Xue *et al.*[57] Aqueous solutions of silver nitrate (5 mM, 2 mL) and sodium citrate (30 mM, 1 mL) were diluted to 100 mL with Milli-Q distilled water and purged under nitrogen for 45 min, while stirrring vigorously. A freshly prepared sodium borohydride solution (50 mM, 1 mL) was added rapidly, initiating a color change to light yellow. Over the next

20 min, additional sodium borohydride (50 mM, 1 mL) and bis-(*p*-sulfonatophenyl)phenylphosphine (5 mM, 1 mL) were added. After 12 h of aging, the pH was raised to 11.00 with 0.2 mM sodium hydroxide. The solutions were irradiated under LEDs of various wavelengths (Rebel LED from Luxeon Star, part number MR-E0070-10S) to achieve nanoprisms of the desired size. Four LEDs were run in series at 0.5 A and around 11 V. The irradiation times were typically around 24 h. Silver nanoprisms with extinction peaks of 480−600 nm were synthesized using this method.

Silica Coating of the Silver Nanoprisms. This was achieved following the protocol by Xue *et al.*[56] A solution of 16-mercaptohexadecanoic acid in ethanol (0.4 mM, 0.05 mL) was added to a 1 mL sample of silver nanoprisms. The nanoprisms were then centrifuged and redispersed into an equal volume of tetraethyl orthosilicate (0.5−1.0 mM in ethanol), with the concentration of tetraethyl orthosilicate controlled to determine approximate silica-shell thickness. Dimethylamine (40 wt %, 0.005 mL) was added and allowed to react for 24 h. The prisms were then centrifuged and redispersed in ethanol. Silica shells of thicknesses varying between 10 and 40 nm were created with this method.

Self-Assembly of Silver Nanoprisms and Polymer Film Processing. For self-assembly of silver nanoprisms on either ITO, glass, or SiO_X and P3HT/PCBM film processing we used the procedure described previously by our group in ref 29. Briefly, the surface of the clean substrates (activated using air plasma) was vapor silanized in a vacuum chamber (80 °C, ∼100 mTorr, 90 min) using 100 μL of 3-aminopropyltrimethoxysilane (APTMS, Sigma-Aldrich). The substrates were immersed in the silver nanoprism solution for 24−48 h. The silver nanoprism films were then transferred to a glovebox (<1 ppm O_2 and H_2O) and overcoated with a 35 nm film of the blend components P3HT (Rieke Metals) and PCBM (Nano-C) (1:1) (15 mg/mL in chlorobenzene, spin coated at 1800 rpm for 1 min). The P3HT:PCBM films were dried in a vacuum chamber overnight.

Device Fabrication. ITO/SiO_X/silver nanoprisms/SiO_X/Al devices for electroabsorption/charge modulation spectroscopy were prepared by thermally depositing a 200 nm layer of SiO_X on ITO using SiO as precursor. The same procedure was used to deposit a second 200 nm layer of SiO_X on top of a silver nanoprism monolayer, on top of which a 100 nm layer of aluminum was thermally evaporated. For ITO/silver nanoprisms/SiO_X/Al devices used for charge modulation spectroscopy an analogous procedure was followed where SiO_X and Al films of 200 and 100 nm thickness, respectively, were thermally deposited. For devices consisting of ITO/supernatant/SiO_X/Al APTMS-treated ITO substrates were immersed for 24 h in the supernatant of colloidal silver nanoprism solutions.

Photoinduced Absorption Spectroscopy (PIA). PIA spectroscopy is a quasi-steady state, pump−probe technique that detects the existence of long-lived excitations (here positive polymer polarons). The apparatus for PIA spectroscopy was designed and assembled in our group. The setup and detection scheme involving standard lock-in techniques are described in detail elsewhere.[29,40] The sample is irradiated with a 200 Hz pump beam (typically 455 or 530 nm) while simultaneously probed with a monochromatic source that can be swept over a large spectral range. The change in transmission (dT) of the sample is detected through a lock-in amplifier, allowing the recording of both "in-phase" (X-channel, shorter-lived carriers) and "out-of-phase" (Y-channel, longer-lived carriers) components.

Charge Modulation Spectroscopy (CMS). CMS is an electro-optical method for the *in situ* characterization of injected charge carriers typically in semiconductor device structures.[42,58] The technique looks specifically at the changes in optical transmission owing to modulation of an external voltage. This allows identification of the spectroscopic signature associated with the voltage-induced dynamic charging/discharging. For charge modulation spectroscopy, monochromated light from a Xe arc lamp was directed on metal−insulator−metal-type device structures. Voltage-modulated transmittance spectra were measured using a Si detector and standard phase-sensitive techniques (see Supporting Information for details). Both the "in-phase" and the "quadrature" component of the lock-in amplifier were recorded, and the phase was referenced to the voltage wave applied to the substrate, corrected for electronic delays. We used a nearest-neighbors averaging algorithm for increasing the signal to noise ratio of our CMS data.

Conflict of Interest: The authors declare no competing financial interest.

Acknowledgment. This paper is based on work supported primarily by ONR, with additional support (J.I.L.C., K.M., EM imaging) from AFOSR. Construction of the CMS apparatus was partially supported by the National Science Foundation (DMR 0449422, DMR 0520567, and DMR 0120967). M.S. acknowledges a fellowship from the Portuguese Foundation for Science and Technology (FCT) (SFRH/BPD/71816/2010). A.H. acknowledges undergraduate salary support from NSF DMR 1005504. Transmission electron microscopy was performed at the NanoTech User Facility (NTUF) at the University of Washington, a member of the NSF National Nanotechnology Infrastructure Network.

Supporting Information Available: Experimental details regarding charge modulation spectroscopy; charge-modulated spectra and corresponding extinction spectra for silver nanoprism samples with resonances throughout the visible spectrum; X- and Y-channel photoinduced absorption spectra for polymer blend films on silver nanoprisms of different size; frequency-modulated photoinduced absorption spectra featuring the lifetimes of the polymer polaron and the electron charge on silver nanoprisms. This material is available free of charge *via* the Internet at http://pubs.acs.org. [†]Present address: National Renewable Energy Laboratory, 15013 Denver West Parkway Golden, Colorado 80401, United States. [‡]Present address: Boeing Research and Technology, Seattle, Washington 98108, United States. [§]Present address: Lawrence Livermore National Laboratory, 7000 East Avenue, Livermore, California 94550. United States. [⊥]Present address: Department of Chemistry, York University, 4700 Keele Street, Toronto, ON, Canada M3J 1P3. A.P. K., M.S., and D.S.G. conceived of the experiments. A.P.K. and M.S. performed the photoinduced absorption experiments. A.H. synthesized the nanoprisms used in the experiments. B.A.M. performed the charge modulation experiments on devices fabricated by M.S. J.I.L.C. and K.M. performed electron microscopy of samples and devices. M.S. and D.S.G. wrote the manuscript. All authors reviewed the final manuscript.

REFERENCES AND NOTES

1. Okamoto, K.; Niki, I.; Shvartser, A.; Narukawa, Y.; Mukai, T.; Scherer, A. Surface-Plasmon-Enhanced Light Emitters Based on InGaN Quantum Wells. *Nat. Mater.* **2004**, *3*, 601–605.
2. Oulton, R.; Sorger, V.; Zentgraf, T.; Ma, R.; Gladden, C.; Dai, L.; Bartal, G.; Zhang, X. Plasmon Lasers at Deep Subwavelength Scale. *Nature* **2009**, *461*, 629–632.
3. Knight, M.; Sobhani, H.; Nordlander, P.; Halas, N. Photodetection with Active Optical Antennas. *Science* **2011**, *332*, 702–704.
4. Anker, J.; Hall, W.; Lyandres, O.; Shah, N.; Zhao, J.; Van Duyne, R. Biosensing with Plasmonic Nanosensors. *Nat. Mater.* **2008**, *7*, 442–453.
5. Chen, Y.; Munechika, K.; Jen-La Plante, I.; Munro, A. M.; Skrabalak, S. E.; Xia, Y.; Ginger, D. S. Excitation Enhancement of CdSe Quantum Dots by Single Metal Nanoparticles. *Appl. Phys. Lett.* **2008**, *93*, 053106.
6. Shen, H.; Bienstman, P.; Maes, B. Plasmonic Absorption Enhancement in Organic Solar Cells with Thin Active Layers. *J. Appl. Phys.* **2009**, *106*, 073109.
7. Anger, P.; Bharadwaj, P.; Novotny, L. Enhancement and Quenching of Single-Molecule Fluorescence. *Phys. Rev. Lett.* **2006**, *96*, 113002.
8. Ming, T.; Chen, H.; Jiang, R.; Li, Q.; Wang, J. Plasmon-Controlled Fluorescence: Beyond the Intensity Enhancement. *J. Phys. Chem. Lett.* **2012**, *3*, 191–202.
9. Munechika, K.; Chen, Y.; Tillack, A. F.; Kulkarni, A. P.; Plante, I. J. L.; Munro, A. M.; Ginger, D. S. Spectral Control of Plasmonic Emission Enhancement from Quantum Dots near Single Silver Nanoprisms. *Nano Lett.* **2010**, *10*, 2598–2603.

10. Tam, F.; Goodrich, G.; Johnson, B.; Halas, N. Plasmonic Enhancement of Molecular Fluorescence. *Nano Lett.* **2007**, *7*, 496–501.
11. Griffo, M.; Carter, S.; Holt, A. Enhanced Photoluminescence of Conjugated Polymer Thin Films on Nanostructured Silver. *J. Lumin.* **2011**, *131*, 1594–1598.
12. Sharma, B.; Frontiera, R.; Henry, A.; Ringe, E.; Van Duyne, R. SERS: Materials, Applications, and the Future. *Mater. Today* **2012**, *15*, 16–25.
13. Willets, K.; Van Duyne, R. Localized Surface Plasmon Resonance Spectroscopy and Sensing. *Annu. Rev. Phys. Chem.* **2007**, *58*, 267–297.
14. Munechika, K.; Chen, Y. C.; Tillack, A. F.; Kulkarni, A. P.; Jen-La Plante, I.; Munro, A. M.; Ginger, D. S. Quantum Dot/Plasmonic Nanoparticle Metachromophores with Quantum Yields That Vary with Excitation Wavelength. *Nano Lett.* **2011**, *11*, 2725–2730.
15. Atwater, H.; Maier, S.; Polman, A.; Dionne, J.; Sweatlock, L. The New "p-n Junction". Plasmonics Enables Photonic Access to the Nanoworld. *MRS Bull.* **2005**, *30*, 385–389.
16. Atwater, H. A.; Polman, A. Plasmonics for Improved Photovoltaic Devices. *Nat. Mater.* **2010**, *9*, 205–213.
17. Albrecht, S.; Schafer, S.; Lange, I.; Yilmaz, S.; Dumsch, I.; Allard, S.; Scherf, U.; Hertwig, A.; Neher, D. Light Management in PCPDTBT:PC70BM Solar Cells: A Comparison of Standard and Inverted Device Structures. *Org. Electron.* **2012**, *13*, 615–622.
18. Peumans, P.; Bulovic, V.; Forrest, S. Efficient Photon Harvesting at High Optical Intensities in Ultrathin Organic Double-Heterostructure Photovoltaic Diodes. *Appl. Phys. Lett.* **2000**, *76*, 2650–2652.
19. Li, X.; Choy, W. C. H.; Huo, L.; Xie, F.; Sha, W. E. I.; Ding, B.; Guo, X.; Li, Y.; Hou, J.; You, J.; Yang, Y. Dual Plasmonic Nanostructures for High Performance Inverted Organic Solar Cells. *Adv. Mater.* **2012**, *24*, 3046–3052.
20. Millstone, J.; Hurst, S.; Metraux, G.; Cutler, J.; Mirkin, C. Colloidal Gold and Silver Triangular Nanoprisms. *Small* **2009**, *5*, 646–664.
21. Standridge, S.; Schatz, G.; Hupp, J. Distance Dependence of Plasmon-Enhanced Photocurrent in Dye-Sensitized Solar Cells. *J. Am. Chem. Soc.* **2009**, *131*, 8407–8409.
22. Kulkarni, A.; Munechika, K.; Noone, K.; Smith, J.; Ginger, D. Phase Transfer of Large Anisotropic Plasmon Resonant Silver Nanoparticles from Aqueous to Organic Solution. *Langmuir* **2009**, *25*, 7932–7939.
23. Lee, J.; Peumans, P. The Origin of Enhanced Optical Absorption in Solar Cells with Metal Nanoparticles Embedded in the Active Layer. *Opt. Express* **2010**, *18*, 10078–10087.
24. Xue, M.; Li, L.; de Villers, B. J. T.; Shen, H. J.; Zhu, J. F.; Yu, Z. B.; Stieg, A. Z.; Pei, Q. B.; Schwartz, B. J.; Wang, K. L. Charge-Carrier Dynamics in Hybrid Plasmonic Organic Solar Cells with Ag Nanoparticles. *Appl. Phys. Lett.* **2011**, *98*, 253302.
25. Chen, F. C.; Wu, J. L.; Lee, C. L.; Hong, Y.; Kuo, C. H.; Huang, M. H. Plasmonic-Enhanced Polymer Photovoltaic Devices Incorporating Solution-Processable Metal Nanoparticles. *Appl. Phys. Lett.* **2009**, *95*, 013305.
26. Kim, K.; Carroll, D. L. Roles of Au and Ag Nanoparticles in Efficiency Enhancement of Poly(3-octylthiophene)/C-60 Bulk Heterojunction Photovoltaic Devices. *Appl. Phys. Lett.* **2005**, *87*, 203113.
27. Kim, S. S.; Na, S. I.; Jo, J.; Kim, D. Y.; Nah, Y. C. Plasmon Enhanced Performance of Organic Solar Cells Using Electrodeposited Ag Nanoparticles. *Appl. Phys. Lett.* **2008**, *93*, 073307.
28. Kim, C.; Cha, S.; Kim, S.; Song, M.; Lee, J.; Shin, W.; Moon, S.; Bahng, J.; Kotov, N.; Jin, S. Silver Nanowire Embedded in P3HT:PCBM for High-Efficiency Hybrid Photovoltaic Device Applications. *ACS Nano* **2011**, *5*, 3319–3325.
29. Kulkarni, A. P.; Noone, K. M.; Munechika, K.; Guyer, S. R.; Ginger, D. S. Plasmon-Enhanced Charge Carrier Generation in Organic Photovoltaic Films Using Silver Nanoprisms. *Nano Lett.* **2010**, *10*, 1501–1505.
30. Lee, J. H.; Park, J. H.; Kim, J. S.; Lee, D. Y.; Cho, K. High Efficiency Polymer Solar Cells with Wet Deposited Plasmonic Gold Nanodots. *Org. Electron.* **2009**, *10*, 416–420.
31. Morfa, A. J.; Rowlen, K. L.; Reilly, T. H.; Romero, M. J.; van de Lagemaat, J. Plasmon-Enhanced Solar Energy Conversion in Organic Bulk Heterojunction Photovoltaics. *Appl. Phys. Lett.* **2008**, *92*, 013504.
32. Rand, B. P.; Peumans, P.; Forrest, S. R. Long-Range Absorption Enhancement in Organic Tandem Thin-Film Solar Cells Containing Silver Nanoclusters. *J. Appl. Phys.* **2004**, *96*, 7519–7526.
33. Stavytska-Barba, M.; Salvador, M.; Kulkarni, A.; Ginger, D. S.; Kelley, A. M. Plasmonic Enhancement of Raman Scattering from the Organic Solar Cell Material P3HT/PCBM by Triangular Silver Nanoprisms. *J. Phys. Chem. C* **2011**, *115*, 20788–20794.
34. Wu, J. L.; Chen, F. C.; Hsiao, Y. S.; Chien, F. C.; Chen, P. L.; Kuo, C. H.; Huang, M. H.; Hsu, C. S. Surface Plasmonic Effects of Metallic Nanoparticles on the Performance of Polymer Bulk Heterojunction Solar Cells. *ACS Nano* **2011**, *5*, 959–967.
35. Yang, J.; You, J. B.; Chen, C. C.; Hsu, W. C.; Tan, H. R.; Zhang, X. W.; Hong, Z. R.; Yang, Y. Plasmonic Polymer Tandem Solar Cell. *ACS Nano* **2011**, *5*, 6210–6217.
36. Chen, X.; Zhao, C.; Rothberg, L.; Ng, M. Plasmon Enhancement of Bulk Heterojunction Organic Photovoltaic Devices by Electrode Modification. *Appl. Phys. Lett.* **2008**, *93*, 123302.
37. Stavytska-Barba, M.; Kelley, A. M. Surface-Enhanced Raman Study of the Interaction of PEDOT:PSS with Plasmonically Active Nanoparticles. *J. Phys. Chem. C* **2010**, *114*, 6822–6830.
38. Wang, D. H.; Kim, D. Y.; Choi, K. W.; Seo, J. H.; Im, S. H.; Park, J. H.; Park, O. O.; Heeger, A. J. Enhancement of Donor–Acceptor Polymer Bulk Heterojunction Solar Cell Power Conversion Efficiencies by Addition of Au Nanoparticles. *Angew. Chem., Int. Ed.* **2011**, *50*, 5519–5523.
39. Topp, K.; Borchert, H.; Johnen, F.; Tune, A. V.; Knipper, M.; von Hauff, E.; Parisi, J.; Al-Shamery, K. Impact of the Incorporation of Au Nanoparticles into Polymer/Fullerene Solar Cells. *J. Phys. Chem. A* **2010**, *114*, 3981–3989.
40. Noone, K.; Anderson, N.; Horwitz, N.; Munro, A.; Kulkarni, A.; Ginger, D. Absence of Photoinduced Charge Transfer in Blends of PbSe Quantum Dots and Conjugated Polymers. *ACS Nano* **2009**, *3*, 1345–1352.
41. MacLeod, B. A.; Horwitz, N. E.; Ratcliff, E. L.; Jenkins, J. L.; Armstrong, N. R.; Giordano, A. J.; Hotchkiss, P. J.; Marder, S. R.; Campbell, C. T.; Ginger, D. S. Built-In Potential in Conjugated Polymer Diodes with Changing Anode Work Function: Interfacial States and Deviation from the Schottky–Mott Limit. *J. Phys. Chem. Lett.* **2012**, *3*, 1202–1207.
42. Ziemelis, K. E.; Hussain, A. T.; Bradley, D. D. C.; Friend, R. H.; Ruhe, J.; Wegner, G. Optical Spectroscopy of Field-Induced Charge in Poly(3-Hexyl Thienylene) Metal-Insulator-Semiconductor Structures - Evidence for Polarons. *Phys. Rev. Lett.* **1991**, *66*, 2231–2234.
43. Bohren, C. F.; Huffman, D. R. *Absorption and Scattering of Light by Small Particles*; Wiley: New York, 1983.
44. Liedtke, M.; Sperlich, A.; Kraus, H.; Baumann, A.; Deibel, C.; Wirix, M.; Loos, J.; Cardona, C.; Dyakonov, V. Triplet Exciton Generation in Bulk-Heterojunction Solar Cells Based on Endohedral Fullerenes. *J. Am. Chem. Soc.* **2011**, *133*, 9088–9094.
45. Noone, K.; Subramaniyan, S.; Zhang, Q.; Cao, G.; Jenekhe, S.; Ginger, D. Photoinduced Charge Transfer and Polaron Dynamics in Polymer and Hybrid Photovoltaic Thin Films: Organic *vs* Inorganic Acceptors. *J. Phys. Chem. C* **2011**, *115*, 24403–24410.
46. Heinemann, M.; von Maydell, K.; Zutz, F.; Kolny-Olesiak, J.; Borchert, H.; Riedel, I.; Parisi, J. Photo-Induced Charge Transfer and Relaxation of Persistent Charge Carriers in Polymer/Nanocrystal Composites for Applications in Hybrid Solar Cells. *Adv. Funct. Mater.* **2009**, *19*, 3788–3795.
47. Botta, C.; Luzzati, S.; Tubino, R.; Bradley, D.; Friend, R. Photoinduced Absorption of Polymer-Solutions. *Phys. Rev. B* **1993**, *48*, 14809–14817.
48. Lucarini, V.; Peiponen, K.-E.; Saarinen, J.; Vartiainen, E. *Kramers–Kronig Relations in Optical Materials Research*; Springer: Berlin, 2005; Vol. 110.

49. Xue, C.; Li, Z.; Mirkin, C. Large-Scale Assembly of Single-Crystal Silver Nanoprism Monolayers. *Small* **2005**, *1*, 513–516.
50. Juluri, B. K.; Zheng, Y. B.; Ahmed, D.; Jensen, L.; Huang, T. J. Effects of Geometry and Composition on Charge-Induced Plasmonic Shifts in Gold Nanoparticles. *J. Phys. Chem. C* **2008**, *112*, 7309–7317.
51. Chapman, R.; Mulvaney, P. Electro-Optical Shifts in Silver Nanoparticle Films. *Chem. Phys. Lett.* **2001**, *349*, 358–362.
52. Daniels, J. K.; Chumanov, G. Spectroelectrochemical Studies of Plasmon Coupled Silver Nanoparticles. *J. Electroanal. Chem.* **2005**, *575*, 203–209.
53. Ung, T.; Giersig, M.; Dunstan, D.; Mulvaney, P. Spectroelectrochemistry of Colloidal Silver. *Langmuir* **1997**, *13*, 1773–1782.
54. Hirakawa, T.; Kamat, P. V. Charge Separation and Catalytic Activity of Ag@TiO2 Core-Shell Composite Clusters under UV-Irradiation. *J. Am. Chem. Soc.* **2005**, *127*, 3928–3934.
55. Banholzer, M.; Harris, N.; Millstone, J.; Schatz, G.; Mirkin, C. Abnormally Large Plasmonic Shifts in Silica-Protected Gold Triangular Nanoprisms. *J. Phys. Chem. C* **2010**, *114*, 7521–7526.
56. Xue, C.; Chen, X.; Hurst, S. J.; Mirkin, C. A. Self-Assembled Monolayer Mediated Silica Coating of Silver Triangular Nanoprisms. *Adv. Mater.* **2007**, *19*, 4071–4074.
57. Xue, C.; Mirkin, C. A. pH-Switchable Silver Nanoprism Growth Pathways. *Angew. Chem., Int. Ed.* **2007**, *46*, 2036–2038.
58. Brown, P. J.; Sirringhaus, H.; Harrison, M.; Shkunov, M.; Friend, R. H. Optical Spectroscopy of Field-Induced Charge in Self-Organized High Mobility Poly(3-hexylthiophene). *Phys. Rev. B* **2001**, *63*, 125204.